Materials Letters 178 (2016) 288–291

Contents lists available at ScienceDirect

Materials Letters

journal homepage: www.elsevier.com/locate/matlet

Camphene effect for morphological change of electrospun SnO_2 nanofibres: From dense to fibre-in-hollow and to hollow nanostructures

Bon.-Ryul Koo [a], Sung.-Tag Oh [b], Hyo.-Jin Ahn [a,b,*]

[a] Program of Materials Science & Engineering, Convergence Institute of Biomedical Engineering and Biomaterials, Seoul National University of Science and Technology, Seoul 139-743, Korea

[b] Department of Materials Science and Engineering, Seoul National University of Science and Technology, Seoul 139-743, Korea

ARTICLE INFO

Article history:
Received 18 March 2016
Received in revised form
28 April 2016
Accepted 5 May 2016
Available online 6 May 2016

Keywords:
SnO_2 nanofibres
Electrospinning
Camphene
Morphological change

ABSTRACT

We fabricated various morphological SnO_2 nanofibres (NFs), which are controlled from dense to fibre-in-hollow and hollow nanostructures, by electrospinning with the introduction of camphene. To control the morphologies of the SnO_2 NFs, the relative loading amounts of camphene to solvent were adjusted to be 0, 50, and 125 wt%. As a result, the SnO_2 NFs formed at 0 wt% camphene showed a dense nanostructure due to the shrinkage effect caused by the thermal decomposition of the polyvinylpyrrolidones. For 50 wt% camphene, the SnO_2 NFs formed the fibre-in-hollow nanostructure because of the occurrence of the Kirkendal effect on the surface of the as-spun SnO_2 NFs. For 125 wt% camphene, the morphology exhibited a hollow nanostructure because of the occurrence of the Kirkendal effect on the entire area of the as-spun SnO_2 NFs. Thus, as the loading amount of camphene was increased, the morphology of the SnO_2 NFs changed from dense to fibre-in-hollow and to hollow.

1. Introduction

One-dimensional (1-D) nanomaterials are gaining popularity in academia and industries because of their unique optical, and electrochemical properties [1]. Recently, various nanostructures of 1-D nanomaterials, such as nanorods and hollow nanostructures, have been developed that combine the fascinating properties of large surface area and high aspect ratio, and have received great interest for use in energy storage devices [1]. In addition, previous studies have used efficient synthetic processes, such as hydrothermal and electrospinning, to fabricate 1 – D nanomaterials [2]. In particular, electrospinning has received increasing attention because of its simple set-up and low-cost characteristics [3]. In addition, SnO_2 is a well-known n-type semiconductor with a wide bandgap (~3.6 eV), which is used in various applications such as electro-optics and energy technologies [4]. Hence, considerable effort has been made to control various morphologies of the SnO_2 NFs by using electrospinning, such as nanobelts and fibre-in-tube nanostructures [3]. However, despite these efforts, the morphological change of SnO_2 NFs obtained by adding camphene has not been investigated. In this study, we fabricated three SnO_2 NF morphologies by electrospinning, in which different loading amounts of camphene were used in a solution, and demonstrated the mechanism of the morphological change of the SnO_2 NFs.

2. Experiments

We fabricated different morphological SnO_2 NFs by using an electrospinning method with camphene. First, the solution of a Sn precursor was prepared by dissolving tin (II) chloride dihydrate ($SnCl_2 \cdot 2H_2O$, Aldrich), polyvinylpyrrolidone (PVP, M_w = 1,300,000 g/mol, Aldrich), and acetic acid (CH_3CO_2H, Aldrich) into N,N-dimethylformamide (C_3H_7NO, Aldrich). The weight percentage of a Sn precursor in the solvent was fixed to 10 wt%. Camphene ((Hill Notation)$C_{10}H_{16}$, Aldrich) was then added to the Sn precursor solution. The relative loading amounts of camphene to the solvent were then adjusted to be 0, 50, and 125 wt% for controlling the morphologies of the SnO_2 NFs. After stirring for 1 h, the prepared solutions were placed in plastic syringes with 23-gauge needles. To obtain SnO_2 NFs through electrospinning, the voltage and distance between a needle tip and collector were taken as ~15 kV and ~20 cm, respectively, and the feeding rate of the solutions was kept at ~0.03 mL/h. The as-spun SnO_2 NFs were calcined at 500 °C for 5 h in air with a heating rate of 15 °C/min,

* Corresponding author.
E-mail address: hjahn@seoultech.ac.kr (H.-J. Ahn).

http://dx.doi.org/10.1016/j.matlet.2016.05.016
0167-577X/

resulting in the formation of the dense (sample A), fibre-in-hollow (sample B), and hollow (sample C) SnO_2 NFs depending on the loading amount of camphene. To investigate the mechanism of the SnO_2 NFs morphological change, the morphological properties of the samples were examined using field-emission scanning electron microscopy (FESEM; Hitachi S-4800) and transmission electron microscopy (MULTI/TEM, Tecnai G^2, KBSI Gwangju Center). The thermal behaviour of the as-spun SnO_2 NFs was characterised by therogravimetric analysis (TGA, TGA-50, Shimadzu).

3. Results and discussion

Fig. 1(a)–(c) and (d)–(f) present the FESEM images of samples A, B, and C before and after the calcination, respectively. In Fig. 1(a)-(c), all the samples show dense 1-D NFs with uniform grey contrast because of the polymeric nature of the PVP and camphene [5]. The diameters of the samples were observed at ~183.1–213.2 nm for sample A, ~174.9–219.2 nm for sample B, and ~182.2–226.5 nm for sample C, implying uniform morphology of as-spun SnO_2 NFs. From FESEM images of SnO_2 NFs calcined at 350 °C (Fig. 1(d)-(f)), the gradual changes in SnO_2 NF morphology with different loading amount of camphene is observed. After calcination at 500 °C, sample A exhibited a dense NF morphology with ~151.0–206.2 nm diameter (Fig. 1(g)). The decrease in diameter of the dense NFs is due to the shrinkage effect induced by thermal decomposition of PVPs [3]. Interestingly, samples B and C, after the calcination (Fig. 1(h) and (i)), formed fibre-in-hollow and

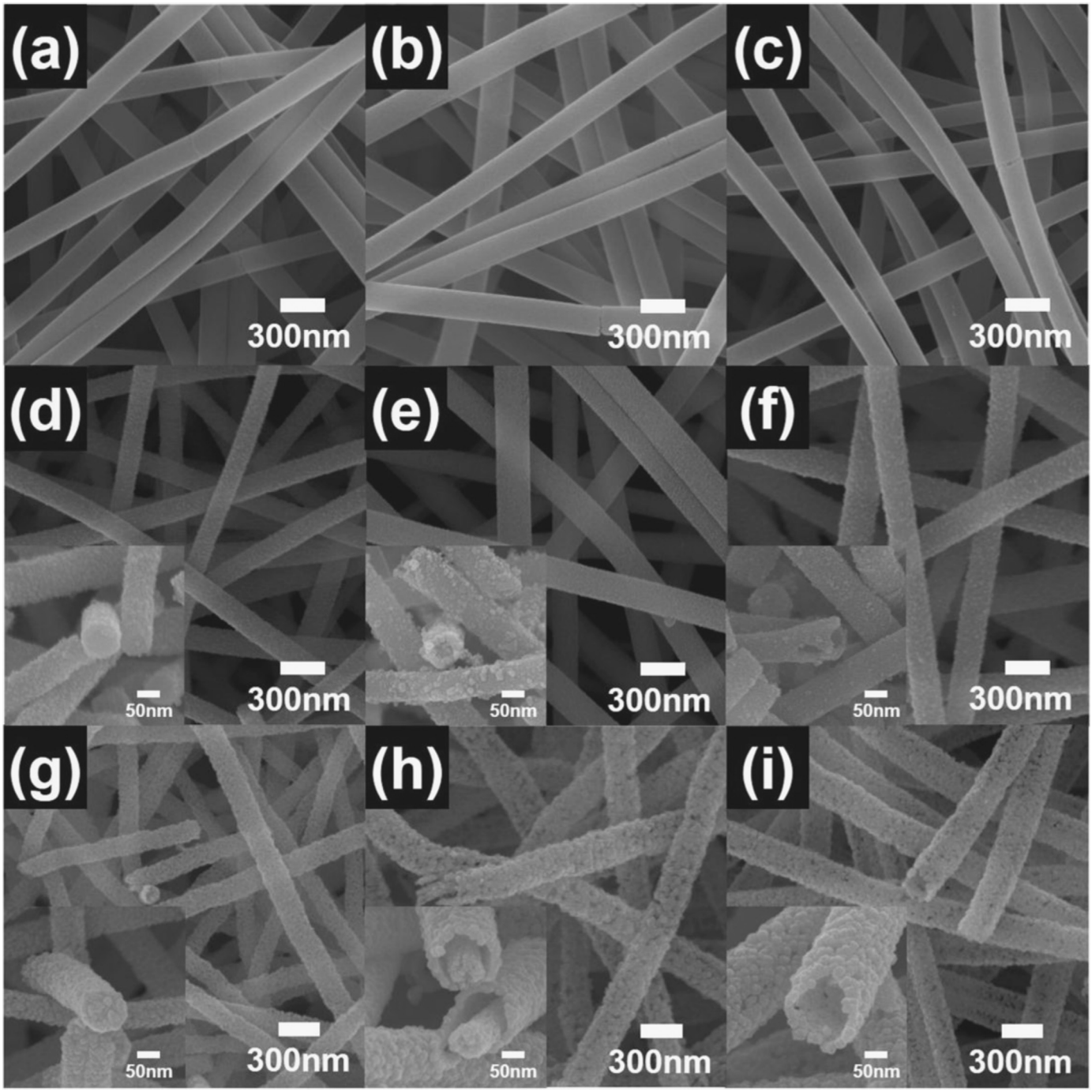

Fig. 1. FESEM images of samples A, B, and C before calcinations (a-c) and after calcinations at 350 °C (d-f) and at 500 °C (g-i), respectively.

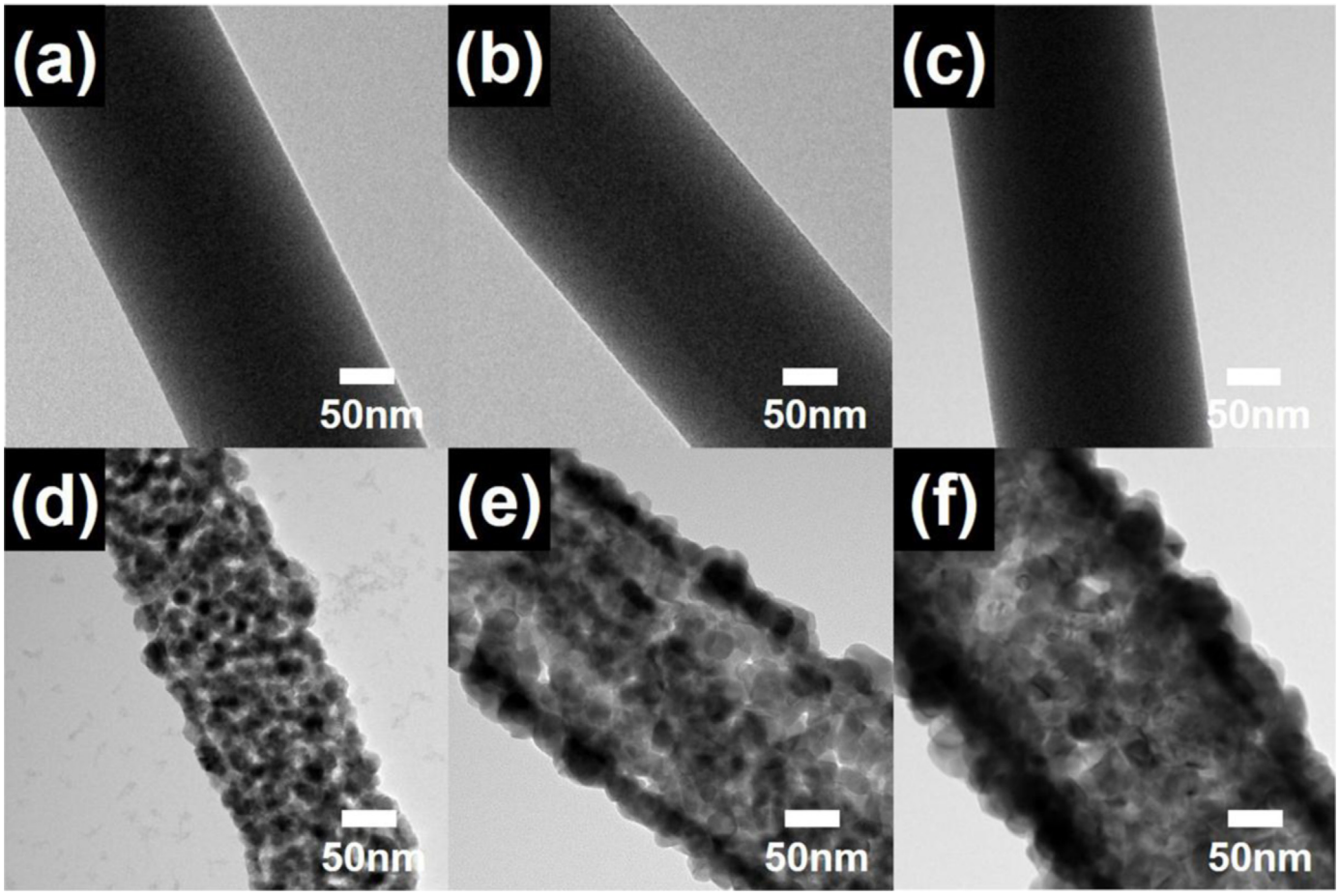

Fig. 2. TEM images of samples A, B, and C obtained before (a-c) and after calcinations (d-f), respectively.

hollow nanostructures with the different loading amounts of camphene (50 and 125 wt%), respectively. In addition, the diameters were ~216.5–286.1 nm for sample B and ~237.1–306.7 nm for sample C, indicating increased diameter values compared to those of the dense NFs (sample A). Therefore, the morphological change of NFs is directly related to the existence of camphene in them. That is, camphene may result in the Kirkendal effect of Sn ions in the NFs because of their low melting temperature (44–48 °C) [5].

To further investigate the different morphological properties of NFs, TEM measurements were carried out. Fig. 2(a)–(c) and (d)–(f) shows the TEM images obtained from samples A, B, and C before and after the calcination, respectively. Fig. 2(a)–(c) shows that all the samples exhibit a uniform dark contrast with similar average diameters of ~198.5 nm for sample A, ~204.6 nm for sample B, and ~199.8 nm for sample C, indicating the formation of the dense as-spun SnO_2 NFs without change in the internal morphology, caused by the camphene, during electrospinning. In contrast, after the calcination, all the samples (Fig. 2(d)–(f)) consisted of nanograins with 8.2–21.7 nm diameter. Furthermore, we observed different contrast distributions among the NFs as the loading amount of camphene increased. That is, sample A exhibited a uniform contrast over the entire area, whereas sample B exhibited a relatively strong dark contrast at the edge and on inner area and relatively bright contrast at the middle. Furthermore, sample C showed a relatively strong dark contrast only at the edge. These results indicate the formation of the dense NFs for sample A, fibre-in-hollow NFs for sample B, and hollow NFs for sample C. Interestingly, the shell thickness of the hollow nanostructures observed in samples B and C is ~33.1–51.8 nm for sample B and ~54.7–72.7 nm for sample C. It means that the shell thickness of sample C is larger than that of sample B. These results may be induced by the diffusion of Sn ions outside the shell region of NFs during calcination. Therefore, the FESEM and TEM results demonstrate that the morphology changed from dense to fibre-in-hollow and hollow NFs with an increase the relative loading amounts of camphene.

We further investigated the mechanism of SnO_2 NF morphological change by performing TGA of the samples at temperatures in the range of 25–600 °C with a heating rate of 15 °C/min (Fig. 3(a)). Sample A displayed a weight loss of 14.8 wt% at 25–280 °C, which indicates the evaporation of the trapped solvent. After a dramatic weight loss at ~300 °C, we observed a continuous weight loss up to ~600 °C. This indicates that SnO_2 NFs shrink because of the thermal decomposition of PVPs [1]. Samples B and C respectively present weight loss of ~21.6% and ~29.7% in the range ~25–280 °C. Compared to sample A, this rapid weight loss is caused by the thermal decomposition of camphene in the as-spun SnO_2 NFs, which accelerates the diffusion of Sn ions outside the NFs. Fig. 3(b) shows the mechanism of SnO_2 NF morphological change. Sample A can cause shrinkage of SnO_2 NFs by thermal decomposition of the PVPs, which leads to the formation of the dense SnO_2 NFs. On the other hand, in samples B and C, the hydrophobic camphene is converted to hydrophilic isobornyl acetate by acetic acid corresponding to the polar aprotic solvent, which results in the coexistence of Sn ions, isobornyl acetate, and PVPs in the as-spun SnO_2 NFs by the electrostatic interaction between Sn ions and their carbonyl oxygen (Fig. 3(c)). Therefore, the thermal decomposition of camphene can accelerate the Kirkendal effect of Sn ions during calcination because of its higher diffusion

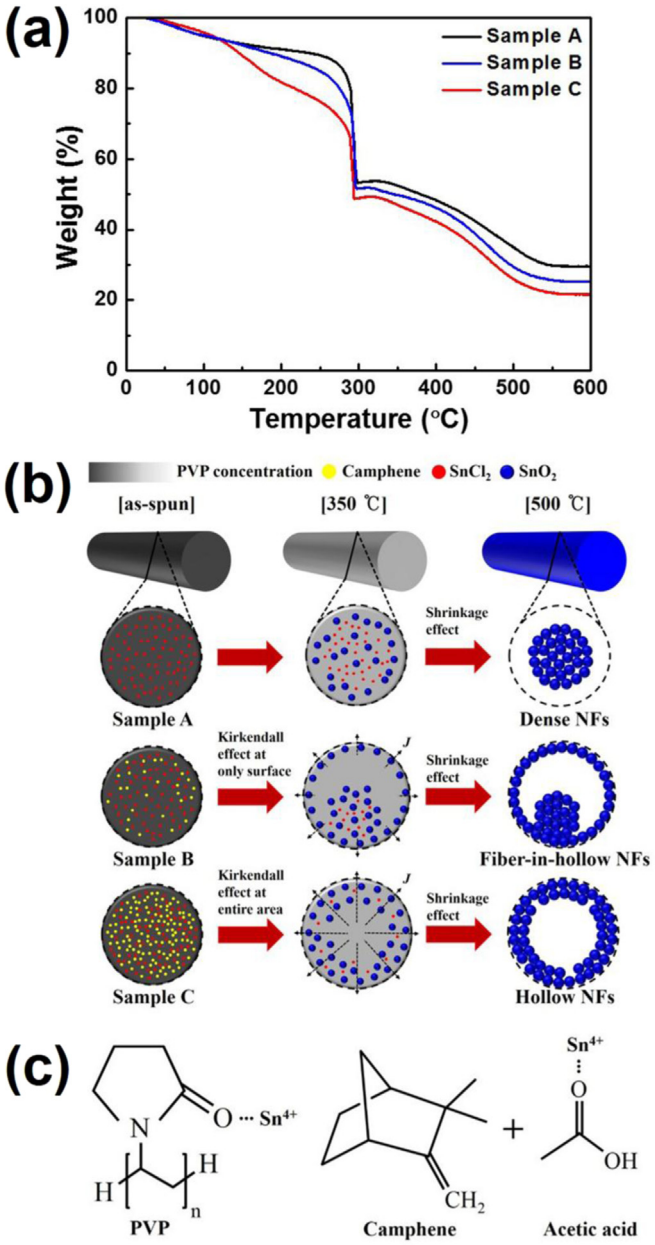

Fig. 3. (a) TGA curves of samples A, B, and C and (b) a schematic diagram of mechanism of SnO_2 NF morphological change by the relative loading amounts of camphene, and (c) molecular structures of PVP, camphene, and acetic acid.

coefficient ($D = \sim 12 \times 10^{-8}\ m^2 s^{-1}$) compared to that of the PVP ($D = \sim 3 \times 10^{-8}\ m^2 s^{-1}$), which is defined as Fick's first law, as the following equation [6]:

$$J = -D(dC/dx)$$

where J is the flux, D is the diffusion coefficient, and dC/dx is the concentration gradient. Sample B generates the Kirkendal effect on the surface of the as-spun SnO_2 NFs because of the small loading amount of camphene, resulting in the formation of the fibre-in-hollow nanostructure. However, in sample C, the Kirkendal effect is fully accelerated on the entire area of the as-spun SnO_2 NFs because of the large loading amount of camphene, resulting in the formation of the hollow nanostructure. In addition, from XRD result (not shown in here), we confirmed that the existence of camphene in the as-spun SnO_2 NFs causes only morphological change after calcination, while not affecting the crystalline structure of SnO_2 NFs. Thus, by fabricating SnO_2 NFs by electrospinning, we can successfully control formation of different morphologies such as dense, fibre-in-hollow, and then hollow nanostructures depending on the relative loading amount of the camphene.

4. Summary

We controlled various morphologies of SnO_2 NFs from dense to fibre-in-hollow and to hollow nanostructures by electrospinning with different loading amounts of the camphene and demonstrated the mechanism of their morphological changes. These results indicated that the dense SnO_2 NFs prepared at 0 wt% camphene was due to the shrinkage effect caused by the decomposition of the PVPs. However, as the loading amount of the camphene was increased, the morphologies of SnO_2 NFs showed the fibre-in-hollow nanostructure at 50 wt% camphene and the hollow nanostructure at 125 wt% camphene, which was due to the Kirkendal effect on the surface and entire area of as-spun SnO_2 NFs, respectively. Therefore, the morphologies of the SnO_2 NFs from dense to fibre-in-hollow and hollow nanostructures was successfully controlled by different loading amounts of camphene.

Acknowledgement

This research was supported by Basic Science Research Program through the National Research Foundation of Korea (NRF) funded by the Ministry of Science, ICT, and Future Planning (NRF-2015R1A1A1A05001252).

References

[1] J. Wu, D. Zeng, X. Wang, L. Zeng, Q. Huang, G. Tang, C. Xie, Langmuir 30 (2014) 11183–11189.
[2] J.G. Lu, P. Chang, Z. Fan, Mater. Sci. Eng. R. 52 (2006) 49–91.
[3] Y.J. Hong, J.W. Yoon, J.H. Lee, Y.C. Kang, Chem. Eur. J. 21 (2015) 371–376.
[4] H.J. Ahn, H.C. Chio, K.W. Park, S.B. Kim, Y.E. Sung, J. Phys. Chem. B 108 (2004) 9815–9820.
[5] B.H. Yoon, Y.H. Koh, C.S. Park, H.E. Kim, J. Am. Ceram. Soc. 90 (2007) 1744–1752.
[6] K.N. Tu, U. Gösele, Appl. Phys. Lett. 86 (2005) 093111.